

Terpene-based eutectic mixtures for cutaneous delivery: Eutectic point vs. molar ratio - which matters more?

Grzegorz S. Czyski^a, Jacob J.K. Kirkensgaard^{b,c}, Stine Rønholt^a, Thomas Rades^{a,*},
Andrea Heinz^{a,*}

^a LEO Foundation Center for Cutaneous Drug Delivery, Department of Pharmacy, University of Copenhagen, Copenhagen 2100, Denmark

^b Department of Food Science, University of Copenhagen, Frederiksberg C DK-1958, Denmark

^c Niels Bohr Institute, University of Copenhagen, Copenhagen Ø DK-2100, Denmark

ARTICLE INFO

Keywords:

Clotrimazole
Deep eutectic solvents
Eutectic point
Stratum corneum
Terpenes
Transdermal delivery

ABSTRACT

Eutectic mixtures (EMs) of small molecules are increasingly used as a platform for dermal and transdermal drug delivery. However, there is still limited knowledge about how their composition impacts their permeation-enhancing effect, with most studies focusing only on formulations corresponding to the eutectic points (EPs) of binary mixtures. To address this, we investigated the role of the EMs' molar composition on their potential as a delivery platform for the model drug clotrimazole (CLOT). We examined several molar ratios of four terpene-based EMs composed of menthol:β-citronellol, thymol:β-citronellol, menthol:camphor and menthol:thymol for their CLOT-solubilizing potential and viscosity. We also studied CLOT skin retention and permeation after applying the CLOT-containing EMs to porcine skin and observed changes in the skin barrier function. For EMs without thymol, the solubility of CLOT in the EMs was independent of the molar ratio between the terpenes. In contrast, the solubility in thymol-based EMs depended on the molar ratio between the terpenes, with the lowest solubilities found for the EMs at their EPs. The viscosity of pure EMs was dictated by their molar composition, and when saturated with CLOT, it was largely governed by the amount of the dissolved drug in the mixtures, also at their EPs. A small amount of CLOT permeated through the porcine skin, with larger quantities of the drug found in the epidermis and, to lesser extent, in the dermis. The amount of CLOT found in the skin did not correlate with the degree of skin impairment and disruption of the lipid packing in the stratum corneum. Importantly, EMs at their EPs did not show better CLOT retention and permeation than the other EMs. Instead, skin retention of CLOT was dependent on the content of terpenes in the EMs, viscosity of the mixtures, and to some extent the drug solubility, rather than a particular ratio between them.

1. Introduction

Deep eutectic solvents and eutectic solvents (also referred to as eutectic mixtures, EMs) have recently gained attention in the pharmaceutical field as promising platforms for small molecules with limited solubility in conventional solvents [1,2]. Although the two terms are often used interchangeably, they should not be considered synonyms. The term EM describes a mixture of two or more components that

exhibits a depression of the melting point (MP) when compared to the MPs of the pure components [3]. This MP depression is attributed to the formation of new hydrogen bonds and van der Waals forces between the constituents [3]. The ratio between the components that results in the greatest depression of the MP is referred to as the eutectic point (EP) of the mixture [4]. On the other hand, the term deep eutectic solvent refers to an EM displaying an unexpected deviation from thermodynamic ideality, leading to an unanticipated “deep” depression of the MP at its

Abbreviations: AsLS, asymmetric least squares; CLOT, clotrimazole; EM, eutectic mixture; EP, eutectic point; HPLC, high performance liquid chromatography; LOD, limit of detection; LOQ, limit of quantification; LPP, long periodicity phase; M:C, menthol:camphor; M:T, menthol:thymol; M:β, menthol:β-citronellol; MeOH, methanol; MP, melting point; PBS, phosphate-buffered saline; RT, room temperature; SAXS, small-angle X-ray scattering; SC, stratum corneum; SG, Savitzky-Golay; SNV, standard normal variate; SPP, short periodicity phase; T:β, thymol:β-citronellol; TEWL, transepidermal water loss; TFA, trifluoroacetic acid; WAXS, wide-angle X-ray scattering.

* Corresponding authors at: Department of Pharmacy, University of Copenhagen, Universitetsparken 2, Copenhagen 2100.

E-mail addresses: thomas.rades@sund.ku.dk (T. Rades), andrea.heinz@sund.ku.dk (A. Heinz).

<https://doi.org/10.1016/j.molliq.2024.125726>

Received 17 April 2024; Received in revised form 26 July 2024; Accepted 7 August 2024

Available online 13 August 2024

0167-7322/© 2024 The Author(s). Published by Elsevier B.V. This is an open access article under the CC BY license (<http://creativecommons.org/licenses/by/4.0/>).

EP [3,4] (Fig. 1). Therefore, deep eutectic solvents should be considered a subclass of EMs [5]. To unify the terminology, we refer to all mixtures that exhibit lower MPs than their individual components as EMs in the present study.

The role of the molar composition, and consequently the MP depression of the formulation for skin permeation has been previously investigated for EMs comprising at least one therapeutic molecule, with the mixtures at their EPs often displaying the highest drug permeation profile [6–9]. Such a dependence has been proposed to result from the inverse correlation between the MP of the permeant and its solubility in the skin lipids [6,10]. A recent, alternative approach involves dissolving a therapeutic compound in an EM formed by at least two other molecules. Such EMs are believed to enhance skin permeation by extracting the skin lipids [11,12]. Several studies have utilized this approach, although only for a single molar ratio of the EMs, often corresponding to their EPs [13–17].

This study aimed to shed light on the influence of the molar composition of terpene-based EMs on drug solubilization and skin permeation processes. Terpenes were chosen as they are known chemical penetration enhancers that affect the skin barrier function by inducing changes in the skin lipid structure [18,19]. In contrast to previous studies, not only did we investigate EMs at their EPs, but also EMs of different terpene compositions. We examined four terpene-based EMs previously described in the literature, namely menthol: β -citronellol (M: β), thymol: β -citronellol (T: β), menthol:camphor (M:C), and menthol:thymol (M:T) [20,21]. The antifungal drug clotrimazole (CLOT) was chosen as a model compound due to its widespread use as a topical agent [22] and limited solubility in aqueous solvents [23]. We assessed the impact of the EM composition on the CLOT solubility, the viscosity of both pure and CLOT-saturated EMs, as well as CLOT skin permeation and retention. We further investigated the effect of the EMs on the skin barrier integrity by measuring changes in the transepidermal water loss (TEWL) after exposure to the EMs. To better understand the impact that EMs have on both the lamellar and lateral lipid arrangement in the skin structure, we recorded small- and wide-angle X-ray scattering (SAXS and WAXS, respectively) patterns of the stratum corneum (SC) after exposure to the EMs [24–29]. Finally, we investigated whether the determined properties of EMs as solvents (solubilizing potential, viscosity,

effect on the skin integrity) influence the retention of CLOT in the skin.

2. Materials and methods

2.1. Materials

CLOT, thymol ($\geq 98.5\%$), (–)-menthol ($\geq 99\%$), (1R)-(+)-camphor (98%), (\pm)- β -citronellol (95%), porcine pancreas trypsin (1000–2000 BAEE units/mg solid), and trifluoroacetic acid (TFA) were purchased from Sigma Aldrich (Schnelldorf, Germany). Phosphate-buffered saline (PBS) tablets were acquired from Fisher Scientific (Geel, Belgium). Soybean trypsin inhibitor (≥ 7000 BAEE units/mg solid) was obtained from Gibco (Grand Island, NY, USA). High performance liquid chromatography (HPLC) grade methanol (MeOH) and ethanol (EtOH) were purchased from VWR (Leuven, Belgium). Purified water was obtained from Millipore Milli-Q Ultrapure Water purification system with a resistivity of 18.2 M Ω at 27.4 °C. Table 1 summarizes the structures, molecular weights, logP values, MPs, and CAS numbers of the compounds utilized in this study.

2.2. Preparation of EMs

Each EM was prepared by combining two terpenes at different molar ratios as presented in Table 2. To prepare the EMs, both terpenes were accurately weighed into a 4 ml glass vial. The mixtures were then left to equilibrate at 40 °C for at least 1 h under constant stirring (600 rpm), until a complete liquefaction of the components was achieved. 40 °C was chosen to ensure that a wide range of EMs of different composition occur in a liquid state and can be investigated. Particular attention was given to EPs of the EMs, i.e., 5:5, 5:5, 6:4, and 6:4 for M: β , T: β , M:C, and M:T, respectively [20,21,35].

2.3. Solubility of CLOT in EMs

The solubility of CLOT in each EM was determined at least in triplicate. An excess amount of CLOT was added to each of the samples described in section 2.2, and they were left to equilibrate at 40 °C for 24 h under constant stirring (600 rpm). The samples were then transferred into 1.5 ml Eppendorf tubes and centrifuged (18000 \times g, 20 min, 40 °C). Thereafter, the supernatants were collected, diluted adequately, and CLOT was quantified using high performance liquid chromatography (HPLC) as specified in section 2.8.

2.4. Viscosity of pure and CLOT-saturated EMs

EMs were prepared as described in section 2.2. The mixtures were divided into two groups: pure and CLOT-saturated. For the CLOT-saturated group, CLOT was added in quantities that matched the average solubility of the drug in these EMs. This step was taken to ensure that the CLOT concentration in the EMs was near their saturation point. The samples were then left to equilibrate at 40 °C for 24 h under constant stirring (600 rpm). Following this, they were visually examined to confirm the complete dissolution of CLOT in the EMs. Rheological measurements of both groups of the mixtures were conducted with an AR-G2 rheometer equipped with a truncated 20 mm cone with a cone angle of 1° and a Peltier plate (TA Instruments, New Castle, USA). The plate temperature was 40 °C. A 10 s pre-shear step was conducted at a shear rate of 100 s⁻¹ followed by 5 min equilibration. Flow curves of three representative molar ratios of each EM (for M: β and T: β : 1:9, 5:5, 8:2; M:T: 2:8, 5:5, 9:1; M:C: 5:5, 7:3, 9:1) were obtained by continuously increasing shear rates from 1 s⁻¹ to 5000 s⁻¹ (four points per decade) over a period of 25 min. Since the curves exhibited Newtonian behavior (Supplementary Fig. 1), all the EMs were concluded to also be Newtonian. Thus, the viscosity of all samples was measured by applying a constant shear rate of 2000 s⁻¹ over one minute (one readout per every 20 s). Three replicates were measured per sample, with an equilibration

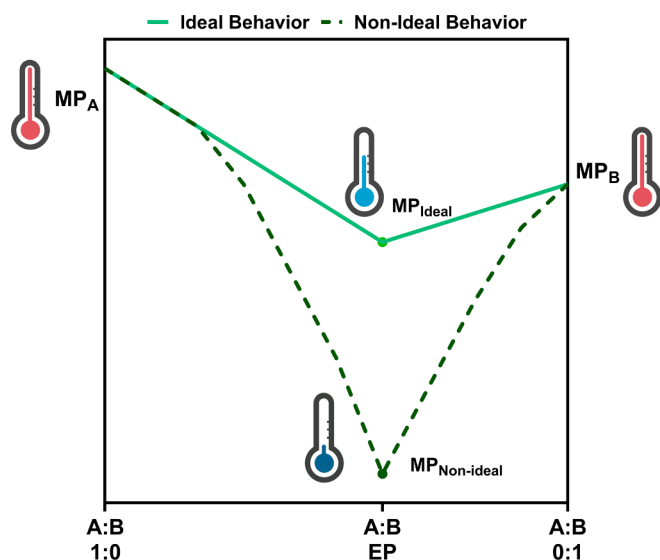
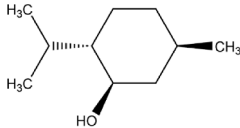
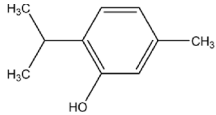
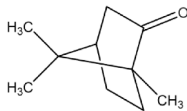
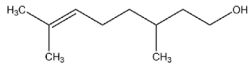
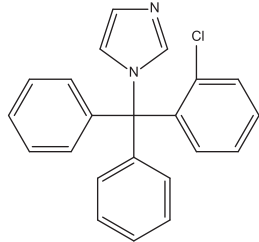


Fig. 1. Exemplary phase diagram of two components with melting points MP_A and MP_B forming a eutectic mixture. Upon mixing, depending on the molar ratio between A and B, the MP of the mixture decreases, following ideal or non-ideal behavior. The latter group of mixtures is often referred to as deep eutectic solvents. The molar ratio with the largest decrease in the MP corresponds to the eutectic point (EP) of the mixture. Created with BioRender.com.

Table 1
List of compounds utilized in the study.

| Molecule | Chemical structure | Molecular weight [g/mol] | logP | MP [°C] | CAS Number | Ref. |
|---------------|---|--------------------------|------|---------|------------|------|
| L-menthol |  | 156.27 | 3.0 | 43 | 2216-51-5 | [30] |
| Thymol |  | 150.22 | 3.3 | 51.5 | 89-83-8 | [31] |
| Camphor |  | 152.23 | 2.2 | 178 | 464-49-3 | [32] |
| β-Citronellol |  | 156.27 | 3.2 | < -80* | 106-22-9 | [33] |
| Clotrimazole |  | 344.84 | 5.0 | 148 | 23593-75-1 | [34] |

* Determined experimentally.

Table 2

EMs of terpenes investigated in the study (light green) with the EPs highlighted (dark green). EMs that did not liquefy completely under the heating and stirring were excluded from the tests and are marked with an "X" (light red).

| EM | Abbreviation | Molar Ratio (Terpene 1 : Terpene 2) | | | | | | | | |
|-----------------------|--------------|-------------------------------------|-----|-----|-----|-----|-----|-----|-----|-----|
| | | 1:9 | 2:8 | 3:7 | 4:6 | 5:5 | 6:4 | 7:3 | 8:2 | 9:1 |
| Menthol:β-citronellol | M:β | ✓ | ✓ | ✓ | ✓ | ✓ | ✓ | ✓ | ✓ | ✗ |
| Thymol:β-citronellol | T:β | ✓ | ✓ | ✓ | ✓ | ✓ | ✓ | ✓ | ✓ | ✗ |
| Menthol:Camphor | M:C | ✗ | ✗ | ✗ | ✗ | ✓ | ✓ | ✓ | ✓ | ✓ |
| Menthol:Thymol | M:T | ✗ | ✓ | ✓ | ✓ | ✓ | ✓ | ✓ | ✓ | ✓ |

step of 5 min between the measurements.

2.5. Preparation of skin samples and permeation studies

Porcine ears were obtained from a local slaughterhouse and rinsed with PBS (pH 7.4 at 25 °C). Intact skin pieces from the outer ears were excised and trimmed to remove hair. The skin samples were then dermatomed (Zimmer Dermatome AN, Zimmer Biomet Denmark, Albertslund, Denmark) to a thickness of ~500 μm and stored at -20 °C prior to permeation experiments.

Permeation studies were carried out using Phoenix Franz diffusion cells (Teledyne Hanson, Chatsworth, CA, USA) with a diffusional surface area of 1 cm². The receptor chambers were filled with 10 ml of degassed EtOH:PBS solution (30:70, v/v) to ensure sufficient solubility of CLOT. Experiments were carried out at 40 °C ± 0.1 °C under constant stirring of the receptor phase (600 rpm). Skin samples were mounted on the diffusion cells with the dermis in direct contact with the receptor phase

and left to equilibrate for 30 min. Next, 100 μl of CLOT-saturated EM was applied to the skin samples in each of the donor chambers, and the samples were covered with parafilm to reduce evaporation. After 24 h, samples of 600 μl were withdrawn from the receptor. The samples were centrifuged (16162 × g, 20 min), and the collected supernatants were subjected to HPLC analysis.

After 24 h, residual EM sample was removed from the skin, and the skin's epidermal side was wiped several times with a dry, and once with an ethanol-wetted cotton swab. The skin samples were left for another 30 min to dry completely, ensuring an adequate condition for the skin integrity testing.

2.6. Skin integrity testing

The effect of the EMs on skin integrity was investigated by measuring the TEWL using an AquaFlux AF200 instrument (Biox, London, UK). The probe was equipped with a coupling part to assess the barrier function

directly from the donor compartment of the Franz cells. Measurements were performed 30 min before applying the formulations to the equilibrated skin samples and 30 min after terminating the permeation studies, once the epidermal side of the skin samples had dried. Each skin piece was measured at least three times.

2.7. Skin retention studies

Heat separation of the epidermis from the dermis was performed after the skin samples had been removed from the Franz cells. The skin pieces were wrapped in aluminum foil and immersed in MilliQ water at 60 °C for 2.5 min, followed by immersing them in MilliQ water at RT for another 45 s. The epidermis was then removed from the dermis with tweezers, and each of the skin layers was transferred into a 5 ml Eppendorf tube, respectively. The separated skin pieces were weighed, and 5 ml of 50:50 MeOH:MilliQ water (v/v) was added to the tubes. The samples were sonicated for 30 min at 30 °C. Subsequently, the samples were left for 24 h at RT under gentle shaking to extract CLOT. Afterwards, 1 ml of the solution was transferred to 1.5 ml Eppendorf tubes and centrifuged (16162 × g, 20 min). The supernatant was collected and subjected to HPLC analysis to quantify the amount of CLOT.

2.8. HPLC analysis

Two different setups, both utilizing an InfinityLab Poroshell 120 EC-C18 column (4.6 mm x 150 mm, 4 μm, Agilent, Santa Clara, CA, USA) equipped with a UHPLC guard (4.6 mm x 5 mm, 4 μm, Agilent, Santa Clara, USA), were used to quantify the CLOT solubility in the EMs and skin permeation and retention.

The solubility of CLOT in the EMs was determined on a Prominence HPLC system (Shimadzu, Kyoto, Japan) with UV detection at 210 nm. An isocratic method with an 80:20 MeOH:MilliQ water (v/v) mixture was employed at a flow rate of 1 ml/min at 30 °C for 8 min. The injection volume was 20 μl, and the retention time of CLOT was ~4.9 min. The limit of detection (LOD) and limit of quantification (LOQ) of the setup were determined to be 2.36 μg/ml and 7.14 μg/ml, respectively.

The content of CLOT in the permeation and retention samples was quantified using a 1260 Infinity II LC system (Agilent, Santa Clara, USA) under gradient conditions. Mobile phase A consisted of 0.1 % (v/v) TFA in MilliQ water, and mobile phase B consisted of 0.1 % (v/v) TFA in MeOH. The gradient was operated at 30 °C and a flow rate of 1 ml/min with the following steps: 0 min – 2 min: 30 % B to 50 % B; 2 min – 9 min: 50 % B to 95 % B; 9 min – 10 min: 95 % B; 10 min – 11 min: 95 % B to 30 % B; 11 min – 14 min: 30 % B. The injection volume was 10 μl, and the retention time of CLOT was ~7.8 min for the UV detection at 210 nm. The LOD and LOQ for this setup were 1.58 μg/ml and 4.78 μg/ml, respectively.

2.9. X-ray diffraction experiments

Prior to X-ray diffraction experiments, porcine SC was separated from the other layers of the skin samples in two consecutive steps. First, heat separation of the epidermis and the dermis was carried out, as described in section 2.7. The epidermis, with the SC facing up, was then placed on filter paper (VWR, Leuven, Belgium), soaked in 0.25 % (w/w) trypsin solution in PBS and incubated for 24 h at 32 °C. Afterwards, the SC was removed from the remaining epidermis with tweezers, rinsed with MilliQ water, submerged in 0.25 % (w/w) trypsin inhibitor solution in PBS to stop activity of trypsin, and rinsed again with MilliQ water.

SC sheets were placed individually in 6-well plates and incubated for 24 h at 40 °C with the CLOT-saturated EMs tested in the permeation and retention studies. A control sample was incubated in PBS under the same conditions. After 24 h, the SC sheets were removed from the wells and blot-dried to remove any excess of the formulations. Each sheet was then loaded into a 1.5 mm borosilicate capillary tube (Hilgenberg GmbH, Malsfeld, Germany) and sealed.

SAXS and WAXS measurements of pure and CLOT-saturated EPs of

the EMs, as well as intact and EM-treated SC were performed with a Nano-inXider instrument (Xenocs SAS, Grenoble, France) with a 40 W micro-focused Cu source producing X-rays with a wavelength of $\lambda = 1.54 \text{ \AA}$. The machine was equipped with a two-detector setup, enabling simultaneous SAXS/WAXS measurements, thus covering scattering wave vectors ($q = 4\pi \sin\theta/\lambda$, where 2θ is the scattering angle) from 0.007 \AA^{-1} to 4.2 \AA^{-1} . The measurements were performed at a medium resolution configuration (50 kV, 0.6 mA, 800 μm beam size, ~80 mph/s flux). Samples were measured for 1 h in vacuum at RT. 2D images were azimuthally averaged to 1D curves of intensity as a function of q . The XSACT software (ver. 2.8, Xenocs SAS, Grenoble, France) was used to subtract the scattering pattern of an empty capillary, and to correct for varying thickness of the sample packed into the capillaries. Curves of the SC were smoothed with a Savitzky–Golay (SG) filter (quadratic polynomial order, 15 points in each sub-model) using Simca software (ver. 18.0.0.372, Sartorius, Göttingen, Germany).

To elucidate the characteristics of peaks in the recorded SC scattering patterns, pretreated regions of interest (SAXS q ranges: 0.05 \AA^{-1} – 0.09 \AA^{-1} and 0.06 \AA^{-1} – 0.20 \AA^{-1} ; WAXS q range: 1.46 \AA^{-1} – 1.65 \AA^{-1}) were subjected to normalization with a standard normal variate (SNV) filter and baseline correction with an asymmetric least squares (AsLS) algorithm (smoothing factor: 10000, asymmetry factor: 0.001) using Simca software. Additionally, the SAXS data were smoothed using a SG filter.

2.10. Statistical analysis

Statistical analysis, linear regressions, and data visualization were performed using Prism GraphPad 10.1.0 (GraphPad, California, USA). In the TEWL experiment, the differences between the samples were evaluated using a two-way ANOVA, followed by Tukey's multiple comparison test. For the solubility, skin permeation and retention data, a one-way ANOVA, followed by Tukey's multiple comparison test, was performed to determine differences. Data are presented as mean ± standard deviation, with p-values below 0.05 indicating significant difference between the groups.

3. Results & discussion

3.1. Effect of molar ratio on properties of terpene-based EMs

To elucidate the impact the molar composition of the EMs has on the solubilizing potential of CLOT, sample viscosity, skin integrity, and skin retention, we determined linear regressions between these variables (see Fig. 2 and Supplementary Fig. 2). Several different dependencies were found between the molar compositions of the EMs and the assessed properties. These dependencies will be discussed in detail in the subsequent sections.

3.1.1. Effect of molar ratio of EMs on CLOT solubility

The solubilities of CLOT in the investigated EMs are shown in Fig. 3 and Supplementary Table 1. Overall, all EMs solubilized substantially more CLOT than water [36], with the highest solubility found for the 2:8 ratio of the T:β EM (274.90±16.10 mg/ml). This is approximately a 345,000-fold increase in comparison to the aqueous solubility of 0.8 μg/ml determined at 40 °C by Saadatfar et al. [36]. Several theories have been proposed to explain the solubilizing potential of EMs, including the hole and the binding theories. The hole theory suggests that the constituents of EMs arrange themselves into a polymer-resembling matrix, with void spaces (holes) accommodating solutes [37]. In contrast, the binding theory proposes that the solute integrates into the molecular network of the EM due to intermolecular interactions, such as hydrogen bonds [38]. However, the most popular theory suggests the formation of hydrogen bonds between the hydrogen bond donor and the hydrogen bond acceptor within the EM [39]. This results in structural heterogeneity within the mixtures, as observed in the WAXS patterns of both pure and CLOT-saturated EMs at their EPs (Supplementary Fig. 3). All four

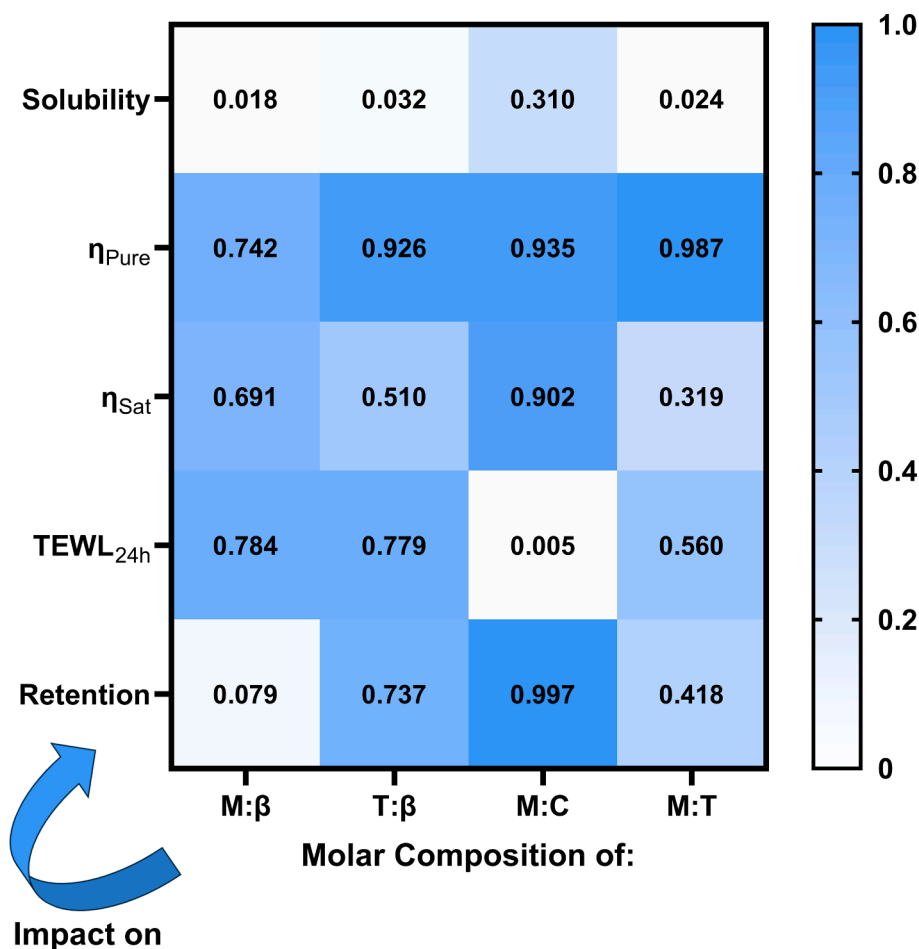


Fig. 2. R^2 values from linear regressions determined between different molar compositions of M:β, T:β, M:C, and M:T EMs and their solubilities, viscosities in pure (η_{Pure}) and CLOT-saturated (η_{Sat}) forms, effect on the skin barrier integrity (TEWL_{24h}), and sum of the CLOT retained in the skin normalized by the mass of each layer., respectively Regression lines of the individual pairs of variables are presented in [Supplementary Fig. 2](#).

EMs exhibited a double peak pattern, implying the formation of molecular clusters and subsequent structural heterogeneity, discussed in more detail in the [Supplementary Materials](#), including [Supplementary Fig. 3](#) and [Supplementary Tables 3 and 4](#). Kaur et al. proposed that this heterogeneity may lead to the presence of high-polarity and low-polarity regions within the EMs, potentially explaining their solubilizing potential [40]. Thus, the solubility of CLOT was much higher in the EMs than in solvents with a continuous hydrogen bond network, such as water [41].

Depending on the terpenes forming the EMs, two different solubility patterns were observed. For the M:β and M:C EMs, the solubility of CLOT was independent of the molar ratio between the terpenes ([Fig. 2](#), [Fig. 3A](#) and [C](#)). Notably, the EMs at their EPs (5:5 and 6:4 for M:β and M:C, respectively) were found to solubilize the drug in a similar fashion to the other EMs. In contrast, the solubility of CLOT in the EMs comprising thymol (T:β and M:T) was dependent on the molar ratio between the terpenes, but not in a linear fashion ([Fig. 2](#), [Fig. 3B](#) and [D](#)). For the T:β EMs, a V-shaped solubility pattern was found, with higher CLOT solubilities found for non-equimolar ratios between thymol and β-citronellol, and the lowest solubility for the equimolar ratio, corresponding to the EP of the mixture. For the M:T EMs a different, W-shaped solubility pattern was identified. The lowest solubilities were found for the 4:6 and 6:4 ratios, with the latter one being the EP of the mixture. A higher disproportion between the molar ratios of menthol and thymol resulted in higher solubility values of the drug in the mixtures, except for the 9:1 ratio.

The presence of thymol in the EMs significantly influenced their

solubilizing potential for CLOT. Thymol, being an asymmetric hydrogen bond donor, induces a strong non-ideal behavior within the formed EMs, leading to a significant depression of their MPs [42–44]. The nonideality of EMs has been suggested to reduce their potential to solvate molecules [5]. This could potentially explain why EMs with molar ratios exhibiting greater deviations from ideality were found to solubilize less CLOT. Consequently, the molar ratios demonstrating the highest degree of nonideality, which corresponds with the EPs of the mixtures, exhibited the lowest solubilizing potential for the drug. In contrast, the EMs lacking thymol exhibit an ideal behavior, and a similar solubilizing potential for CLOT was observed across the assessed molar ratios. However, further research is needed to confirm this potential dependency.

In summary, EPs of the ideal EMs solubilized CLOT to a similar extent as the other molar ratios. In contrast, EPs of the non-ideal EMs showed lower solubilities of the drug than the other molar ratios.

3.1.2. Effect of molar ratio of EMs on their viscosity

The viscosities of both pure and CLOT-saturated EMs are presented in [Fig. 3](#) and [Supplementary Tables 5 and 6](#).

Generally, EMs without CLOT showed low viscosities with values below 20 mPa s. The highest viscosity was found for the M:T EM (18.02 ± 0.18 mPa s for the 9:1 ratio), whereas the lowest viscosity was determined for the T:β EM (5.72 ± 0.08 mPa s for the 1:9 ratio). A linear dependence was observed between the molar ratio of the mixtures and their viscosity ([Fig. 2](#)). The viscosities of T:β EMs increased with increasing content of thymol in the mixtures, whereas the viscosities of

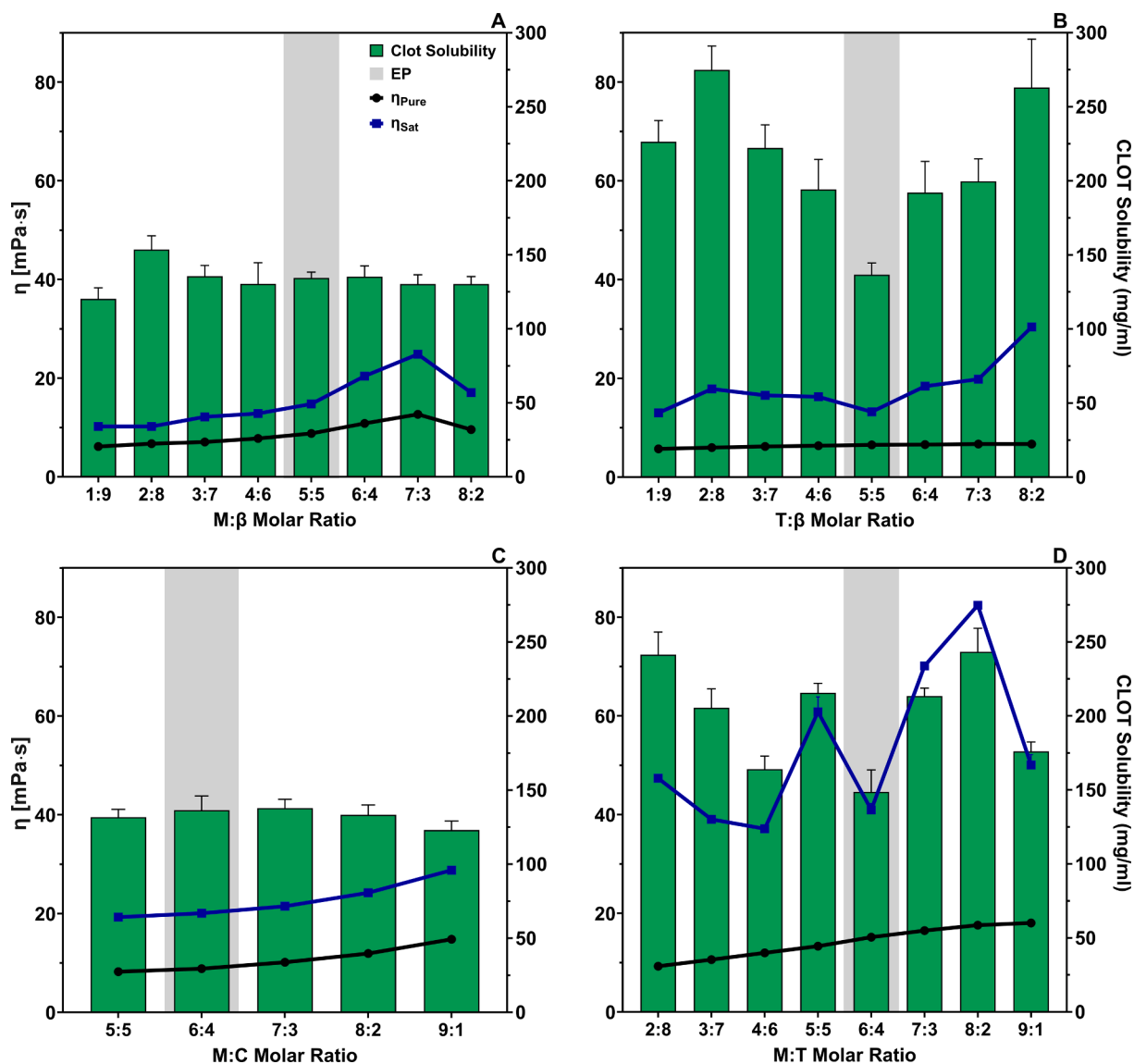


Fig. 3. Solubility of CLOT in different EMs and viscosities of pure (η_{pure}) and CLOT-saturated (η_{sat}) formulations for (A) M:β, (B) T:β, (C) M:C, and (D) M:T, respectively. Values were determined at 40 °C (n = 3–6). The EPs of the EMs are highlighted in grey. P values indicating statistically significant difference between the solubilities are presented in [Supplementary Table 2](#).

M:β, M:C, and M:T EMs increased with increasing content of menthol (Fig. 3A–D). This is in line with previous reports, where a similar trend was observed for M:C and M:T EMs [45,46]. Deepika et al. suggested that the cyclohexyl chair structure of menthol leads to an increase in the frictional motions in the liquid, in contrast to the planar phenyl ring of thymol, thus resulting in a higher viscosity of the mixtures [46]. Importantly, the EPs of the EMs made no noticeable exception from the observed trends.

Saturation of the EMs with CLOT significantly altered their viscosities. Overall, the highest viscosity was found for the 8:2 ratio of the M:T system (82.44 ± 0.24 mPa s). Depending on the terpene pair, two distinct viscosity patterns were observed. For thymol-free EMs, the addition of CLOT increased their viscosity consistently across all mixtures, while mirroring the linear dependence between the viscosity and molar ratio, as observed for their drug-free forms (Fig. 2, Fig. 3A and C). This is due to similar solubility values and, consequently, the amount of drug dissolved in the EMs. Notably, the viscosity at the EPs of these mixtures did not deviate from this trend. Saturation of thymol-rich EMs with CLOT also increased their viscosity, but the dependence between the viscosity and molar ratio was no longer linear, as observed for their pure

counterparts. Instead, the viscosity was tied to the amount of CLOT dissolved in the mixtures, echoing the patterns found in the solubility studies (Fig. 3B and D). Higher viscosities were found for EMs with higher CLOT solubility. Conversely, EMs with lower solubilizing potential exhibited lower viscosities. Both EPs of the mixtures displayed low viscosities due to the lower drug solubilities found at these ratios.

Several studies have observed an increasing viscosity of the solution with an increasing concentration of solutes, including trehalose, sucrose, glycerol, pectin, or monoclonal antibodies [47–49]. Yadav et al. suggested that increasing the concentration of a solute results in higher demands for the energy needed to interact with the solute in solution, causing the raise of viscosity [50]. This could explain the similarity between the solubility and viscosity patterns.

Overall, the viscosity of EMs is primarily dictated by their molar composition. However, for drug-saturated EMs, the viscosity is largely governed by their solubilizing potential. Importantly, the EPs of the mixtures, whether in pure or drug-saturated forms, consistently follow these trends and they do not deviate from the trends observed for the other molar ratios.

Based on the solubility profiles and distinct rheological behaviors,

three to four EMs (including EPs) from each of the terpene pairs were chosen and their effect on the skin integrity, followed by their potential as dermal and transdermal delivery platforms was explored.

3.1.3. Effect of molar ratio of EMs on skin integrity

The TEWL is widely used to assess the level of skin integrity [51,52], and its change after contact with the EMs is presented in Fig. 4. Overall, all EMs significantly compromised the skin barrier function, as evidenced by the increase of TEWL after 24 h of exposure to the EMs. The results are consistent with other studies that showed an impairment of the skin barrier, i.e., an increase in TEWL, of skin treated with menthol [53,54], thymol [55], and camphor [56].

The degree of skin impairment was influenced by the molar ratio between the terpenes. Both M:β and M:T EMs exhibited a linear dependence between the degree of skin impairment and molar ratios of the mixtures with increasing molar ratios of menthol in the mixtures corresponding to overall lower TEWL readouts (Fig. 2, Fig. 4A and D). The EPs of the mixtures (5:5 and 6:4 for M:β and M:T EMs, respectively) showcased a similar level of skin impairment as the other ratios.

An opposite trend was noted for the T:β EMs, where an increase of thymol amount correlated with a higher degree of skin impairment (Fig. 2, Fig. 4B). The EP (5:5) of the mixture led to a significantly stronger impairment of the skin than the 3:7 ratio, but it was similar to the effect observed for the 7:3 ratio. No dependence was observed between the TEWL and molar ratios of M:C EMs, although the mixture at its EP (6:4) showed the strongest effect on the skin impairment (Fig. 2, Fig. 4C). However, the effect was not significantly different from the 9:1 ratio.

According to the TEWL data, none of the EMs at their EPs demonstrated a distinct effect on skin barrier function compared to the other tested EMs.

3.1.4. Effect of molar ratio of EMs on skin permeation and retention

The impact of EMs on the skin permeation and retention of CLOT is summarized in Fig. 5. Since the EMs were saturated with CLOT, the thermodynamic activity of the drug dissolved in the mixtures reached its maximum [57]. Thus, the permeation and retention rates of CLOT across the EMs should be similar, provided the EMs do not affect the skin absorption. This was indeed the case for the skin permeation (Fig. 5A1–D1). However, for skin retention, several differences were found among the EMs (Fig. 5A2–D2 and A3–D3). This suggests that the composition of the EMs, i.e., the molar ratio between the terpenes, influenced the drug retention.

For the M:β EMs, no linear dependence was found between the molar ratio of the terpenes and the amounts of CLOT retained in the skin (Fig. 2, Fig. 5A4). The EM at its EP (5:5) was found to retain significantly less drug in the epidermis than at the 3:7 ratio (Fig. 5A2), with a similar dermal retention between the mixtures (Fig. 5A3). In contrast, an increase of the amount of thymol in the T:β EMs correlated with a higher CLOT retention in the skin (Fig. 2, Fig. 5B4). Furthermore, at the 7:3 ratio, the mixture retained significantly more drug in the epidermis and the dermis than at the remaining ratios (Fig. 5B2 and B3). A different trend was observed for the M:C EMs, where an increase of menthol was linearly correlated with lower skin retention (Fig. 2, Fig. 5C4). Notably, the EM at its EP (6:4) led to the highest drug retention in the dermis (Fig. 5C3). Finally, all M:T EMs were found to lead to CLOT retention in both the epidermis and the dermis to a similar extent (Fig. 5D2 and 5D3) and a weak linear dependence was observed between the variables (Fig. 2).

The EMs at their EPs showcased several distinct effects on skin retention in comparison to the other EMs, including significantly higher dermal retention for the M:C, lower epidermal retention for the M:β and T:β, and similar retention for the M:T. This suggests that the rate of

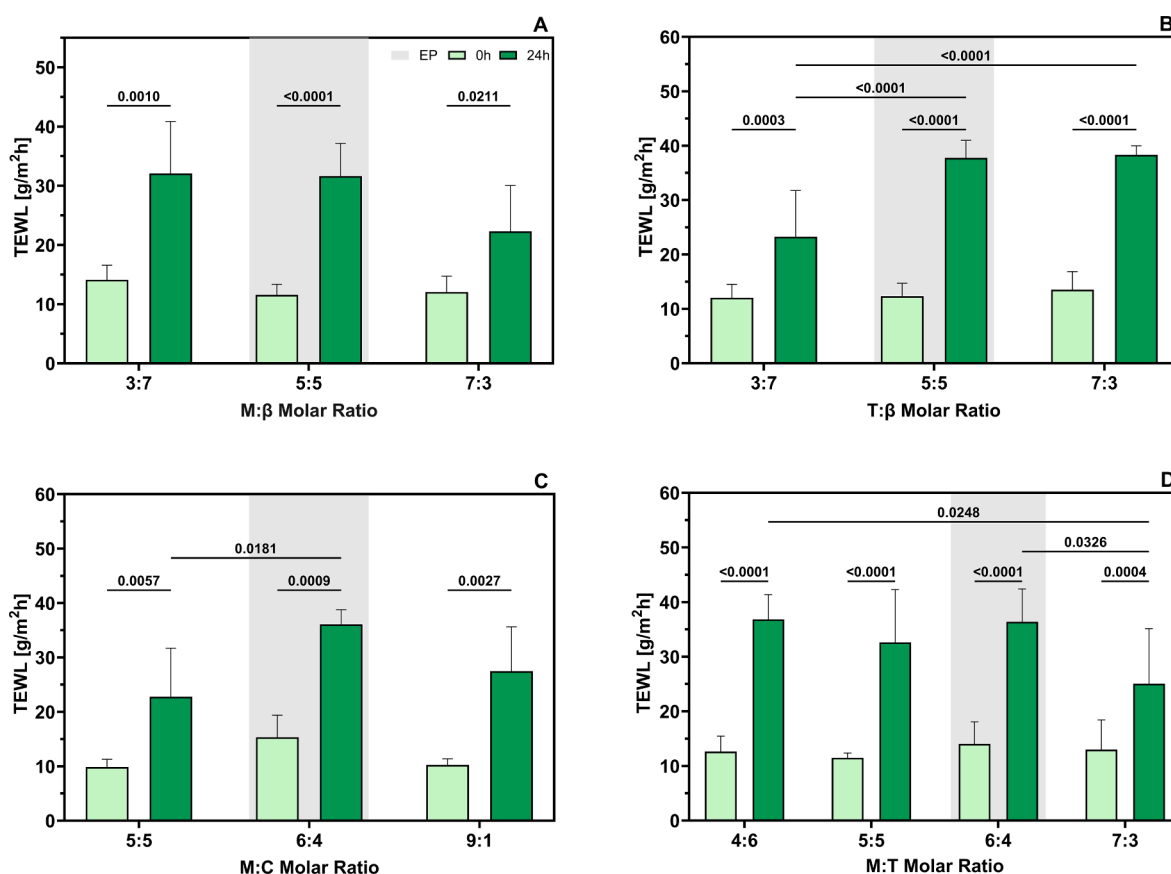


Fig. 4. TEWL of porcine skin measured prior to application (0 h) and 24 h after application of the (A) M:β, (B) T:β, (C) M:C, and (D) M:T EMs, respectively (n = 3–5). EMs corresponding to the EPs are highlighted in grey. P values of statistical significance between the samples are highlighted.

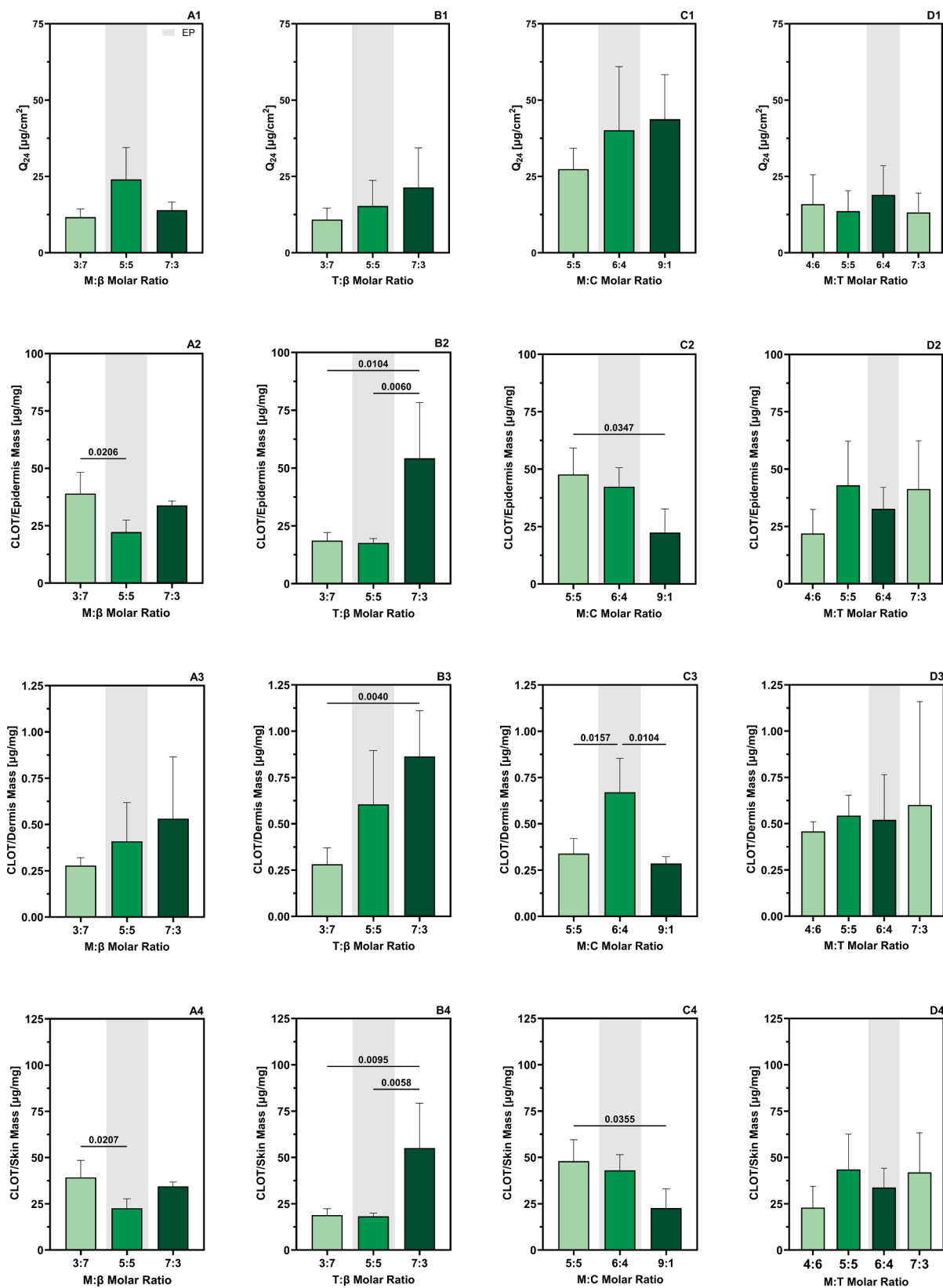


Fig. 5. Effect of the (A) M: β , (B) T: β , (C) M:C, and (D) M:T EMs on the permeation (Q_{24} , A1–D1) and retention of CLOT in the epidermis (A2–D2) and the dermis (A3–D3), respectively, followed by a sum of CLOT found in the skin (A4–D4) after a 24 h experiment performed at 40 °C ($n = 3-5$). The quantity of CLOT detected in the skin was normalized to the mass of the respective layer from which the drug was extracted. EMs at the EPs are highlighted in grey, and p values of statistical significance between the groups are shown.

retention depends on the physicochemical properties of the mixtures used as a delivery platform, rather than a particular ratio of terpenes in the EM.

3.1.5. Effect of molar ratio of EMs on lipid arrangement in SC

To elucidate the effect of EMs on the lipid arrangement in the skin, SAXS and WAXS patterns of the SC sheets treated with CLOT-saturated EMs, as well as the SC sheets treated with PBS (control), were recorded (Figs. 6 and 7).

The structure of the intact SC is composed of corneocytes embedded in a lipid matrix, acting as the physical barrier of the skin [29]. The lipids are organized in two often coexisting lamellar structures – one with a long repeat distance of ~ 13.40 nm, called the long periodicity phase (LPP), and one with a short repeat distance of ~ 6.40 nm, called the short periodicity phase (SPP) [26,29]. Within these lamellar structures, a lateral arrangement of the hydrocarbon chains of the lipids is present [28,29]. For porcine skin, a hexagonal lateral arrangement has been identified, corresponding to a distance d of ~ 4.1 Å between the lipid chains [28].

The SAXS pattern of the PBS-incubated SC showed a series of diffraction peaks (Fig. 6, black line). The first peak at $q \sim 0.09$ Å⁻¹ (a) corresponds to the first-order diffraction peak of the SPP ($d = 2\pi n/0.09$ Å⁻¹ ≈ 6.40 nm for $n = 1$) [26,29]. The second peak at $q \sim 0.14$ Å⁻¹ (b) corresponds to the

third-order diffraction peak of the LPP ($d = 2\pi n/0.14$ Å⁻¹ ≈ 13.40 nm for $n = 3$) [26,29].

All tested EMs affected the lamellar structure of the SC, in general causing the disappearance of the diffraction peaks a and b, suggesting a disruption of the SPP and LPP. However, a few exceptions were noted. Treatment with the T:B EM at the 3:7 ratio gave rise to a single broad diffraction peak (Fig. 6B3). The peak shifted towards a lower q range, indicating LPP swelling and consequently increased d -spacing between the lamellae as described previously [26,58]. For the 9:1 ratio of M:C and all M:T EMs, a new diffraction peak appeared at $q \sim 0.075$ Å⁻¹ (Fig. 6C2 and D2), suggesting either SPP swelling or formation of a new lamellar structure between the components of the EM and the SC [26].

The WAXS patterns of the PBS-treated SC sheets (Fig. 7, black lines) revealed several diffraction peaks, originating from different structures in the SC. The leftmost peak at $q \sim 0.64$ Å⁻¹ (c), corresponding to a distance of 9.89 Å, is related to the corneocytes present in the SC [28]. The peak at $q \sim 1.27$ Å⁻¹ (d), corresponding to a distance of 4.96 Å, is composed of the overlapping scattering vectors of the secondary β -sheet structure of keratin and the fluid packing of the SC lipids [25,28]. The peak present at $q \sim 1.52$ Å⁻¹ (e), corresponding to a distance of 4.12 Å, originates from the hexagonal lateral packing of the skin lipids [25,28,29,59]. Additionally, a broad diffraction peak with its peak intensity at $q \sim 2.00$ Å⁻¹ (f) corresponds to water present in the sample,

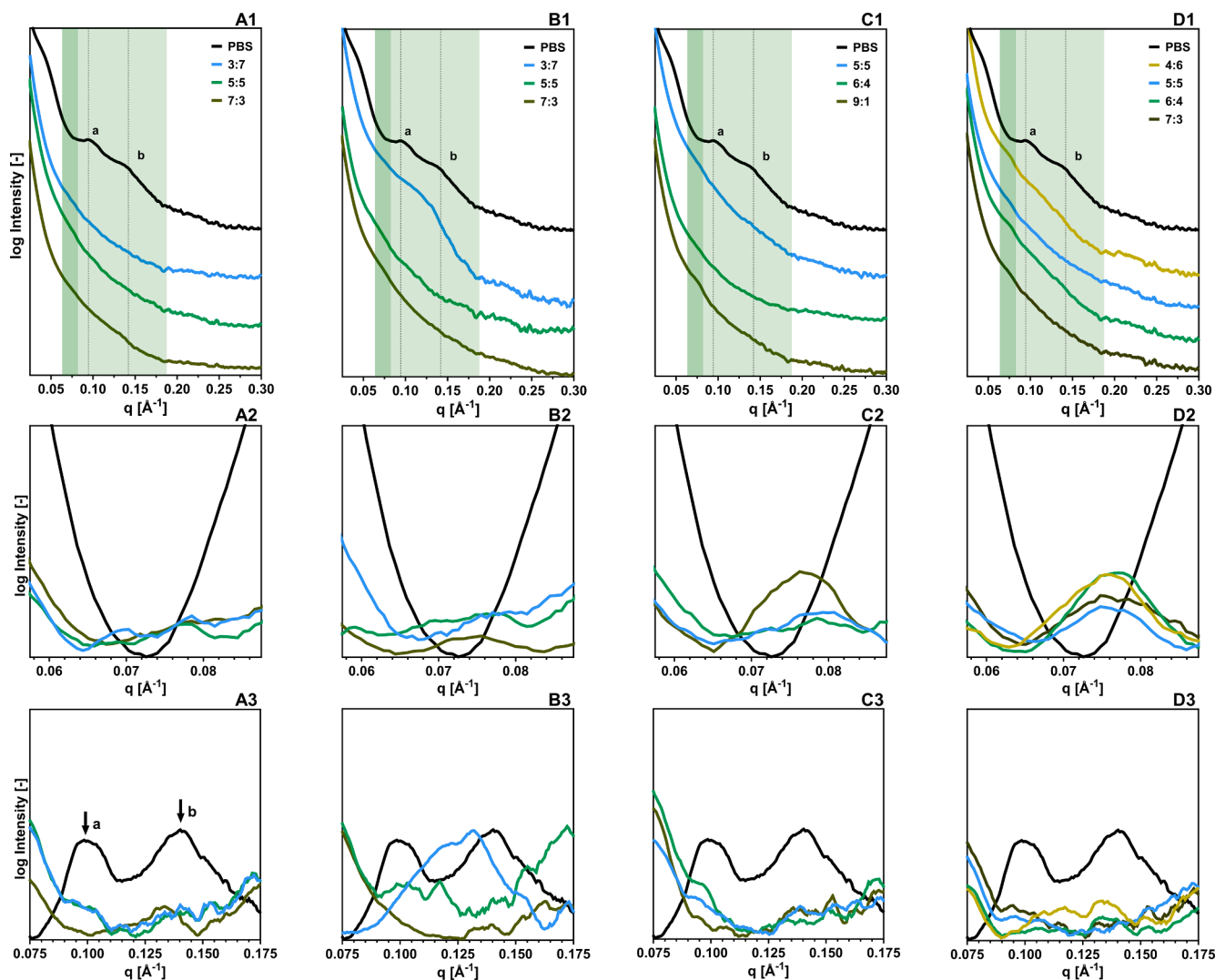


Fig. 6. SAXS patterns of isolated SC sheets treated with PBS and the (A1) M:β, (B1) T:β, (C1) M:C, and (D1) M:T EMs, respectively, at RT. The first-order diffraction peak of the SPP (a), and the third-order diffraction peak of the LPP (b) are indicated by dashed lines. The patterns are offset for clarity. Q regions with substantial changes in the scattering patterns of the lipid arrangement (dark and light green) were subjected to SNV, AsLS, and SG treatments (A2–D2, A3–D3).

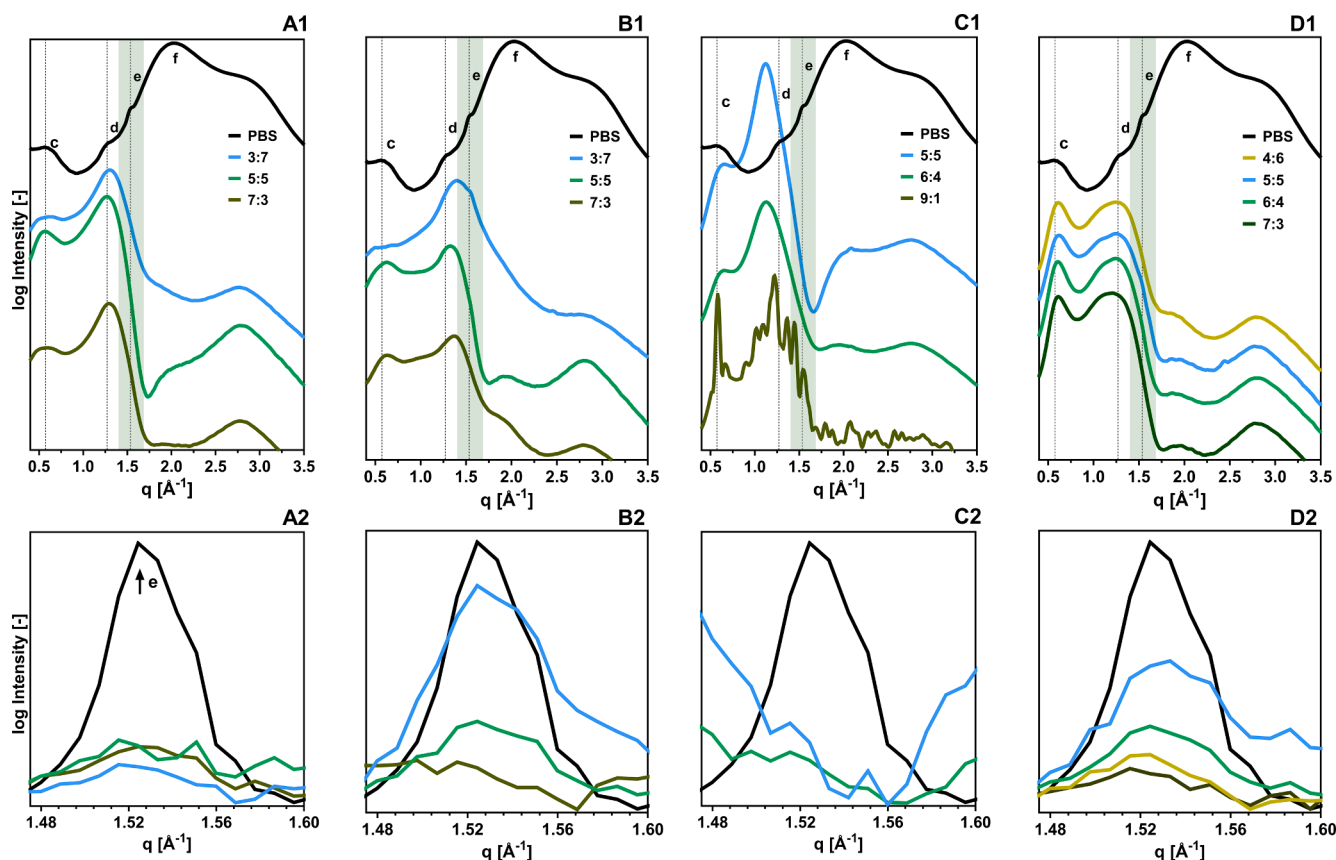


Fig. 7. WAXS patterns of isolated SC sheets treated with PBS and the (A1) M:β, (B1) T:β, (C1) M:C, and (D1) M:T EMs, respectively, at RT. The (c) keratin interchain distance, (d) combination of secondary β-sheet structure of keratin and the fluid lipid chain packing, (e) hexagonal lipid chain packing, and (f) water for the PBS-treated SC samples are highlighted in the patterns. The patterns are offset for clarity. Q regions with substantial changes in the scattering pattern of the lipid arrangement (light green) were subjected to SNV and AsLS treatments (A2–D2). The WAXS pattern of the SC treated with the 9:1 ratio of M:C was impossible to analyze due to the crystallization of menthol during the measurement (C1).

indicating a high hydration state of the intact SC [28].

According to the WAXS data, all EMs led to a dehydration of the SC confirmed by a decrease in the intensity of the f peak [28]. Since the diffraction peaks of the EMs overlapped with the keratin-derived peaks (c and d), the analysis was focused on the effect of the EMs on the organization of the SC lipids. Based on the changes in the scattering patterns, two categories of EMs were distinguished, those causing complete disappearance of the hexagonal packing (M:B, M:C EMs), and those with varying impact on the lipid lateral packing dependent on the applied EM (T:B, M:T EMs).

In the case of T:B EMs (Fig. 7B1 and 7B2), higher amounts of thymol caused a larger disarrangement of the hexagonal packing, expressed by changes in its peak intensities. The 3:7 EM had the least impact on the lateral organization, which is in agreement with the preserved lamellarity seen in the SAXS curve (Fig. 6B1 and B3). These observations correlate well with the TEWL measurements, indicating that the water loss increase was due to the impairment of the lipid packing. At the same time, the most disruptive effect on the lipid organization was seen for the 7:3 ratio mixture, translating to the highest retention profile.

A distinct effect on the lipid packing arrangement was found for the M:T EMs (Fig. 7D1 and D2). The degree of lateral disarrangement varied between the molar ratios but was not related to the amount of either thymol or menthol in the mixtures. Moreover, the degree of arrangement did not correlate with the other results – the largest diffraction peak was found for the 5:5 ratio mixture, even though its effect on the TEWL and skin retention was similar to the remaining molar ratios. In contrast, for the 7:3 ratio mixture, the hexagonal packing was completely disrupted, and yet its impact on the TEWL was significantly lower than for the 4:6 and 6:4 EMs.

Taken together, EMs at their EPs affected the lamellar and lateral packings of the SC lipids in a fashion similar to the other EMs. Terpenes are considered to increase skin penetration predominantly due to their effect on the skin lipids [18]. For instance, they have been shown to form hydrogen bonds with ceramide headgroups, disrupting their tight packing [18,26]. Furthermore, EMs may also affect CLOT retention through extraction of the skin lipids. Such a phenomenon was observed by Araki et al. for thymol- and menthol-based EMs, where decreasing intensities of the SPP and LPP peaks in the SAXS patterns and distinct Fourier-transform infrared spectra were observed, suggesting lipid extraction and membrane fluidization [17].

The concentration of applied terpenes should also be considered when interpreting the data. Even though the terpenes are perceived as generally safe chemicals [19], they are still toxic to living organisms [60]. Thus, they have been used as penetration enhancers in low concentrations, usually ranging between 1 % and 10 % [18,19]. Therefore, application of pure terpenes on the skin, as in the present study, might affect the skin barrier function differently than their diluted forms. Moghadam et al. observed only minor changes in the WAXS profiles of the SC upon contact with low concentrations of menthol and camphor (1 % w/w in PG), suggesting a fluidizing effect on the membrane [26]. In contrast, Cornwell et al. found a significant disruption of the lamellar structures upon application of terpenes as oils and saturated solutions, according to SAXS data [58]. The authors further suggested the formation of terpene-based pools between the intercellular lipids. This effect may potentially explain the presence of a new diffraction peak in the SAXS patterns for some EMs in this study.

3.2. Effect of solvent-related properties of EMs on skin retention

In addition to their molar composition, the impact of EMs on the skin retention may be influenced by the properties of these mixtures as solvents. Thus, to elucidate the impact of the CLOT solubility, EM viscosity in both pure and CLOT-saturated forms, and skin impairment on the drug retention, linear regressions between these parameters and the amount of CLOT retained in the skin were carried out (Fig. 8, Supplementary Fig. 4).

For the M:β EMs, the skin retention of CLOT was independent of their solubilizing potential and viscosities, regardless of whether they were in pure or drug-saturated forms (Fig. 8). Furthermore, an increase in skin impairment did not correspond to increased skin retention. Using the EM at its EP (5:5 ratio) led to less CLOT retention in the skin than for the 3:7 EM, even though both had a similar impact on TEWL (Fig. 4A, Fig. 5A). This suggests that skin impairment is not the sole mechanism involved in CLOT retention. Despite disrupting both the lamellar and lateral lipid arrangements in the SC, the mixtures affected skin integrity differently, as shown by changes in TEWL.

The solubilities of CLOT in the T:β EMs did not have an influence on the extent of skin retention (Fig. 8). On the other hand, the viscosity of pure and CLOT-saturated EMs was positively correlated with skin retention. However, since an increase in thymol content also correlated with higher skin retention (Fig. 2), the apparent effect of viscosity on retention may be due to the effect of thymol. Changes in the skin barrier function, i.e., TEWL, did not influence the skin retention of CLOT (Fig. 8). Despite showing similar TEWL values (Fig. 4B), the application of the EM at its EP (5:5 ratio) and the 7:3 EM resulted in significantly different amounts of CLOT retained in the skin (Fig. 5B).

Higher solubilities of CLOT in the M:C EMs were associated with higher CLOT retention. In contrast, higher viscosities of both the

unsaturated and saturated forms of the EMs correlated with lower amounts of CLOT found in the skin, indicating an impact of the viscosity on skin retention (Fig. 8). However, the solubilities were somewhat dependent on the EMs' viscosities, as shown in Supplementary Fig. 5. Since the viscosity was also a factor affecting CLOT retention, it could partly explain the observed correlation between the solubility and retention. Moreover, the amount of menthol in the mixtures was also inversely correlated with the drug retention (Fig. 2). Thus, the impact of the viscosities of these EMs on the retention remains questionable. The amount of retained CLOT was not dependent on the TEWL, i.e., the skin impairment (Fig. 8). Similar retention profiles were found for both EMs with high (5:5 ratio) and low (EP, 6:4 ratio) TEWL values (Fig. 4C, Fig. 5C). However, all tested EMs led to complete disarrangement of the SC lipids (Fig. 6C3, Fig. 7C3).

Finally, the solubility of CLOT in the M:T EMs was positively correlated with the retention of CLOT in the skin. Moreover, an increase in the viscosity of CLOT-saturated EMs was also correlated with higher skin retention of CLOT (Fig. 8). The dependence of retention on solubility may be due to the relationship between CLOT solubility and viscosity, similar to the M:C EMs (Supplementary Fig. 5). Furthermore, higher TEWL values were slightly correlated with lower dermal retention. EMs that had a strong impact on skin impairment (5:5 and 6:4 (EP) ratios) preserved some level of lipid arrangement in the SC (Fig. 6D3, Fig. 7D3). In contrast, those with a weaker impact (7:3 ratio) significantly disrupted lipid packing.

Overall, the identified correlations suggest that the effect of the EMs on the skin retention of CLOT is influenced by the properties of the mixtures as solvents, such as their viscosities (T:β, M:C, M:T EMs) and, to a certain extent, the drug solubilities in the EMs (M:C, M:T). Notably, the EPs of the mixtures are not an exception from the trends described for the other tested EMs.

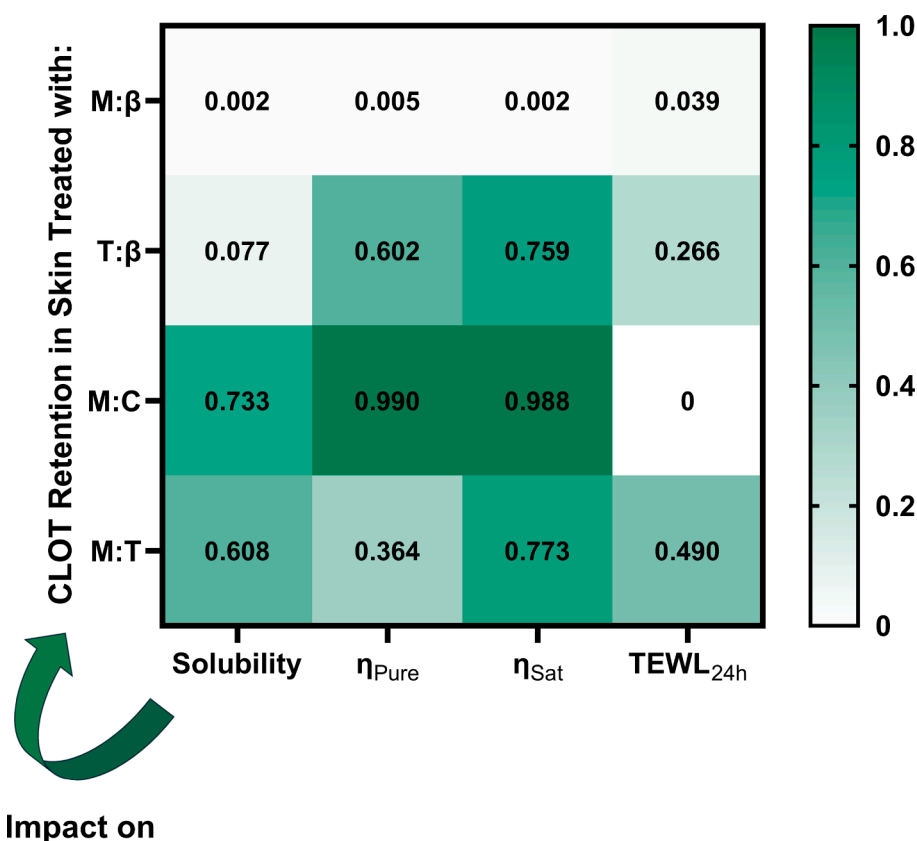


Fig. 8. R^2 values from linear regressions determined between the solubilities, viscosities in pure (η_{Pure}) and CLOT-saturated (η_{Sat}) forms of the M:β, T:β, M:C, and M:T EMs, respectively, as well as their effect on the skin barrier integrity (TEWL_{24h}) and the sum of CLOT retention in skin treated with the EMs (normalized by the mass of each layer). Regression lines of the individual pairs of variables are presented in Supplementary Fig. 4.

4. Conclusion

In this study, we demonstrate that terpene-based EMs are promising solvents for water-insoluble drug CLOT, confirming their potential for topical delivery. The results indicate that the EMs at their EPs exhibit similar, and in the case of thymol-based EMs, lower solubilizing potential than other EMs. The viscosity of pure EMs is linearly correlated with the molar ratios between the terpenes, while their CLOT-saturated forms show a dependence of the viscosity on the amount of the dissolved drug. Furthermore, the EMs primarily impair the skin barrier through disarrangement of the skin lipids in the SC. Notably, EMs at their EPs do not show a superior effect on skin impairment or CLOT retention compared to the other tested EMs. Instead, the extent of skin retention is influenced by the content of individual terpenes and their action as penetration enhancers, as well as the inherent properties of the mixtures, such as their viscosity, and to some extent CLOT solubility. However, the high content of pure terpenes used to form EMs carries the risk of irritation and toxicity-related events upon application on the skin, limiting their potential as a realistic and feasible transdermal delivery platform. Therefore, further research is needed to develop and characterize formulations with lower terpene content, possibly by introducing skin-friendly co-solvents, and to assess their performance as potential transdermal delivery platforms.

Declaration of generative AI in scientific writing

During the preparation of this work, the authors used OpenAI's GPT-4 model, also known as Microsoft Copilot, to enhance text clarity, ensure transparency, and perform grammar checks. After using this tool/service, the authors reviewed and edited the content as needed and take full responsibility for the content of the publication.

CRediT authorship contribution statement

Grzegorz S. Czyski: Writing – original draft, Methodology, Investigation, Formal analysis, Conceptualization. **Jacob J.K. Kirkensgaard:** Writing – review & editing, Methodology, Formal analysis. **Stine Rønholt:** Writing – review & editing, Methodology. **Thomas Rades:** Writing – review & editing, Supervision, Project administration, Funding acquisition, Formal analysis, Conceptualization. **Andrea Heinz:** Writing – review & editing, Supervision, Project administration, Formal analysis, Conceptualization.

Declaration of competing interest

The authors declare that they have no known competing financial interests or personal relationships that could have appeared to influence the work reported in this paper.

Data availability

Data will be made available on request.

Acknowledgements

The authors would like to acknowledge the Drug Delivery and Biophysics of Biopharmaceuticals group, Department of Pharmacy, University of Copenhagen for providing access to an HPLC instrument. Data were generated by accessing research infrastructure of the University of Copenhagen, including FOODHAY (Food and Health Open Innovation Laboratory, Danish Roadmap for Research Infrastructure).

Funding

The work was supported by LEO Foundation grants LF-ST-21-500005 Project 1 (GSC, TR) as well as LF15007 (AH, SR).

Appendix A. Supplementary data

Supplementary data to this article can be found online at <https://doi.org/10.1016/j.molliq.2024.125726>.

References

- [1] Z. Li, P.I. Lee, Investigation on drug solubility enhancement using deep eutectic solvents and their derivatives, *Int J Pharm* 505 (2016) 283–288, <https://doi.org/10.1016/j.ljpharm.2016.04.018>.
- [2] H. Palmelund, M.P. Andersson, C.J. Asgreen, B.J. Boyd, J. Rantanen, K. Löbmann, Tailor-made solvents for pharmaceutical use? Experimental and computational approach for determining solubility in deep eutectic solvents (DES), *Int J Pharm X* 1 (2019) 100034, <https://doi.org/10.1016/j.jpx.2019.100034>.
- [3] B.B. Hansen, S. Spittle, B. Chen, D. Poe, Y. Zhang, J.M. Klein, A. Horton, L. Adhikari, T. Zelovich, B.W. Doherty, B. Gurkan, E.J. Maginn, A. Ragauskas, M. Dadmun, T.A. Zawodzinski, G.A. Baker, M.E. Tuckerman, R.F. Savinell, J. R. Sangoro, Deep Eutectic Solvents: A Review of Fundamentals and Applications, *Chem Rev* 121 (2021) 1232–1285, <https://doi.org/10.1021/ACS.CHEMREV.0C00385>.
- [4] T. El Achkar, H. Greige-Gerges, S. Fourmentin, Basics and properties of deep eutectic solvents: a review, *Environ Chem Lett* 19 (2021) 3397–3408, <https://doi.org/10.1007/S10311-021-01225-8>.
- [5] D.O. Abranches, J.A.P. Coutinho, Everything You Wanted to Know about Deep Eutectic Solvents but Were Afraid to Be Told, *Annu Rev Chem Biomol Eng* 14 (2023) 141–163, <https://doi.org/10.1146/ANNUREV-CHEMBOENG-101121-085323/CITE/REFWORKS>.
- [6] P.W. Stott, A.C. Williams, B.W. Barry, Transdermal delivery from eutectic systems: enhanced permeation of a model drug, ibuprofen, *Journal of Controlled Release* 50 (1998) 297–308, [https://doi.org/10.1016/S0168-3659\(97\)00153-3](https://doi.org/10.1016/S0168-3659(97)00153-3).
- [7] F. Al-Akayleh, S. Adwan, M. Khanfer, N. Idkaidek, M. Al-Remawi, A Novel Eutectic-Based Transdermal Delivery System for Risperidone, *AAPS PharmSciTech* 22 (2021) 1–11, <https://doi.org/10.1208/S12249-020-01844-4>.
- [8] X. Yuan, A.C. Capomacchia, Influence of Physicochemical Properties on the In Vitro Skin Permeation of the Enantiomers, Racemate, and Eutectics of Ibuprofen for Enhanced Transdermal Drug Delivery, *J Pharm Sci* 102 (2013) 1957–1969, <https://doi.org/10.1002/JPS.23548>.
- [9] S. Mohammadi-Samani, G. Yousefi, F. Mohammadi, F. Ahmadi, Meloxicam transdermal delivery: effect of eutectic point on the rate and extent of skin permeation, *Iran J Basic Med Sci* 17 (2014) 112./pmc/articles/PMC3976748/ (accessed January 4, 2024).
- [10] S. Chakraborty, J.H. Chormale, A.K. Bansal, Deep eutectic systems: An overview of fundamental aspects, current understanding and drug delivery applications, *Int J Pharm* 610 (2021) 121203, <https://doi.org/10.1016/j.ljpharm.2021.121203>.
- [11] Q.M. Qi, M. Duffy, A.M. Curreri, J.P.R. Balkaran, E.E.L. Tanner, S. Mitragotri, Q. M. Qi, A.M. Curreri, J.P.R. Balkaran, E.E.L. Tanner, S. Mitragotri, M. Duffy, Comparison of Ionic Liquids and Chemical Permeation Enhancers for Transdermal Drug Delivery, *Adv Funct Mater* 30 (2020) 2004257, <https://doi.org/10.1002/ADFM.202004257>.
- [12] E.E.L. Tanner, K.N. Ibsen, S. Mitragotri, Transdermal insulin delivery using choline-based ionic liquids (CAGE), *Journal of Controlled Release* 286 (2018) 137–144, <https://doi.org/10.1016/j.jconrel.2018.07.029>.
- [13] M. Sakuragi, H. Yoshimura, K. Kusakabe, Effects of structures of microemulsions containing a deep eutectic solvent on the entrapment amount and the skin permeation of resveratrol, *Jpn J Appl Phys* 59 (2020) 035002, <https://doi.org/10.35848/1347-4065/AB6B74>.
- [14] Q. Shen, X. Li, W. Li, X. Zhao, Enhanced intestinal absorption of daidzein by borneol/menthol eutectic mixture and microemulsion, *AAPS PharmSciTech* 12 (2011) 1044–1049, <https://doi.org/10.1208/S12249-011-9672-4>.
- [15] M.C. Gohel, S.A. Nagori, Resolving Issues of Content Uniformity and Low Permeability Using Eutectic Blend of Camphor and Menthol, *Indian J Pharm Sci* 71 (2009) 622, <https://doi.org/10.4103/0250-474X.59543>.
- [16] C. Liu, J. Hu, H. Sui, Q. Zhao, X. Zhang, W. Wang, Enhanced skin permeation of glabridin using eutectic mixture-based nanoemulsion, *Drug Deliv, Transl Res* 7 (2017) 325–332, <https://doi.org/10.1007/S13346-017-0359-6>.
- [17] Y. Araki, Y. Hamada, N. Imamura, K. Yamasaka, M. Sakuragi, Evaluation of terpene-based hydrophobic deep eutectic solvents as skin permeation enhancers, *Jpn J Appl Phys* 62 (2023) 015003, <https://doi.org/10.35848/1347-4065/ACB392>.
- [18] J. Chen, Q.D. Jiang, Y.P. Chai, H. Zhang, P. Peng, X.X. Yang, Natural Terpenes as Penetration Enhancers for Transdermal Drug Delivery, *Molecules* 2016, Vol. 21, Page 1709 21 (2016) 1709. <https://doi.org/10.3390/MOLECULES21121709>.
- [19] M. Aqil, A. Ahad, Y. Sultana, A. Ali, Status of terpenes as skin penetration enhancers, *Drug Discov Today* 12 (2007) 1061–1067, <https://doi.org/10.1016/J.DRUDIS.2007.09.001>.
- [20] M.A.R. Martins, L.P. Silva, N. Schaeffer, D.O. Abranches, G.J. Maximo, S.P. Pinho, J.A.P. Coutinho, Greener Terpene-Terpene Eutectic Mixtures as Hydrophobic Solvents, *ACS Sustain Chem Eng* 7 (2019) 17414–17423, <https://doi.org/10.1021/ACSUSCHEMENG.9B04614>.
- [21] C. Fan, Y. Liu, T. Sebbah, X. Cao, C. Fan, Y. Liu, T. Sebbah, X. Cao, A Theoretical Study on Terpene-Based Natural Deep Eutectic Solvent: Relationship between Viscosity and Hydrogen-Bonding Interactions, *Global Challenges* 5 (2021) 2000103, <https://doi.org/10.1002/GCH2.202000103>.

- [22] J.L. Soriano-Ruiz, A.C. Calpena-Capmany, C. Cañadas-Enrich, N.B. de Febrer, J. Suñer-Carbó, E.B. Souto, B. Clares-Naveros, Biopharmaceutical profile of a clotrimazole nanoemulsion: Evaluation on skin and mucosae as anticandidal agent, *Int J Pharm* 554 (2019) 105–115, <https://doi.org/10.1016/j.ljpharm.2018.11.002>.
- [23] G. Balata, M. Mahdi, R. Bakera, Improvement of Solubility and Dissolution Properties of Clotrimazole by Solid Dispersions and Inclusion Complexes, *Indian J Pharm Sci* 73 (2011) 517, <https://doi.org/10.4103/0250-474X.98995>.
- [24] S.H. White, D. Mirejovsky, G.I. King, Structure of Lamellar Lipid Domains and Corneocyte Envelopes of Murine Stratum Corneum. An X-ray Diffraction Study¹, *Biochemistry* 27 (1988) 3725–3732, <https://doi.org/10.1021/B100410A031>.
- [25] J. Doucet, A. Potter, C. Baltenneck, Y.A. Domanov, Micron-scale assessment of molecular lipid organization in human stratum corneum using microprobe X-ray diffraction, *J Lipid Res* 55 (2014) 2380–2388, <https://doi.org/10.1194/jlr.M053389>.
- [26] S.H. Moghadam, E. Saliya, S.D. Wettig, C. Dong, M.V. Ivanova, J.T. Huzil, M. Foldvari, Effect of chemical permeation enhancers on stratum corneum barrier lipid organizational structure and interferon alpha permeability, *Mol Pharm* 10 (2013) 2248–2260, <https://doi.org/10.1021/MP300441C>.
- [27] S. Perticaroli, J.L. Meyers, F.C. Wireko, O. Akintelure, J.T. Webber, R.T. Cambron, S. Vierling, S.R. Sealschott, K.S. Wei, E. Smith, P.J. Ray, Cleansers' mildness: Stratum corneum lipid organization and water uptake after a single wash, *Journal of Raman Spectroscopy* 51 (2020) 795–806, <https://doi.org/10.1002/JRS.5841>.
- [28] E.H. Mojumdar, Q.D. Pham, D. Topgaard, E. Sparr, Skin hydration: interplay between molecular dynamics, structure and water uptake in the stratum corneum, *Scientific Reports* 2017 7:1 7 (2017) 1–13, <https://doi.org/10.1038/s41598-017-15921-5>.
- [29] J.A. Bouwstra, M. Ponc, The skin barrier in healthy and diseased state, *Biochimica et Biophysica Acta (BBA) - Biomembranes* 1758 (2006) 2080–2095, <https://doi.org/10.1016/j.bbame.2006.06.021>.
- [30] l-Menthol | C10H20O | CID 16666 - PubChem, (n.d.). <https://pubchem.ncbi.nlm.nih.gov/compound/l-Menthol> (accessed November 1, 2023).
- [31] Thymol | C10H14O | CID 6989 - PubChem, (n.d.). <https://pubchem.ncbi.nlm.nih.gov/compound/Thymol#section=Non-Human-Toxicity-Values> (accessed November 1, 2023).
- [32] Camphor (synthetic) | C10H16O | CID 159055 - PubChem, (n.d.). <https://pubchem.ncbi.nlm.nih.gov/compound/159055> (accessed November 1, 2023).
- [33] beta-CITRONELLOL, (+/-) | C10H20O | CID 8842 - PubChem, (n.d.). <https://pubchem.ncbi.nlm.nih.gov/compound/8842> (accessed November 1, 2023).
- [34] Clotrimazole | C22H17ClN2 | CID 2812 - PubChem, (n.d.). <https://pubchem.ncbi.nlm.nih.gov/compound/2812> (accessed November 1, 2023).
- [35] A. Alhadid, L. Mokrushina, M. Minceva, Formation of glassy phases and polymorphism in deep eutectic solvents, *J Mol Liq* 314 (2020) 113667, <https://doi.org/10.1016/j.molliq.2020.113667>.
- [36] F. Saadatfar, A. Shayanfar, E. Rahimpour, M. Barzegar-Jalali, F. Martinez, M. Bolourtchian, A. Jouyban, Measurement and correlation of clotrimazole solubility in ethanol + water mixtures at T = (293.2 to 313.2) K, *J Mol Liq* 256 (2018) 527–532, <https://doi.org/10.1016/j.molliq.2018.02.068>.
- [37] Y.H. Choi, J. van Spronsen, Y. Dai, M. Verberne, F. Hollmann, I.W.C.E. Arends, G. J. Witkamp, R. Verpoorte, Are Natural Deep Eutectic Solvents the Missing Link in Understanding Cellular Metabolism and Physiology? *Plant Physiol* 156 (2011) 1701–1705, <https://doi.org/10.1104/PP.111.178426>.
- [38] Y. Liu, J.B. Friesen, J.B. McAlpine, D.C. Lankin, S.N. Chen, G.F. Pauli, Natural Deep Eutectic Solvents: Properties, Applications, and Perspectives, *J Nat Prod* 81 (2018) 679–690, <https://doi.org/10.1021/ACS.JNATPROD.7B00945>.
- [39] W. Lu, H. Chen, Application of deep eutectic solvents (DESs) as trace level drug extractants and drug solubility enhancers: State-of-the-art, prospects and challenges, *J Mol Liq* 349 (2022) 118105, <https://doi.org/10.1016/j.molliq.2021.118105>.
- [40] S. Kaur, A. Gupta, H.K. Kashyap, Nanoscale Spatial Heterogeneity in Deep Eutectic Solvents, *Journal of Physical Chemistry B* 120 (2016) 6712–6720, <https://doi.org/10.1021/ACS.JPCB.6B04187>.
- [41] M. Busato, G. Mannucci, V. Di Lisio, A. Martinelli, A. Del Giudice, A. Tofoni, C. Dal Bosco, V. Migliorati, A. Gentili, P. D'Angelo, Structural Study of a Eutectic Solvent Reveals Hydrophobic Segregation and Lack of Hydrogen Bonding between the Components, *ACS Sustain Chem Eng* (2022), <https://doi.org/10.1021/ACSSUSCHEMENG.2C00920>.
- [42] D.O. Abranches, J.A.P. Coutinho, Type V deep eutectic solvents: Design and applications, *Curr Opin Green Sustain Chem* 35 (2022) 100612, <https://doi.org/10.1016/j.cogsc.2022.100612>.
- [43] D.O. Abranches, M.A.R. Martins, L.P. Silva, N. Schaeffer, S.P. Pinho, J.A. P. Coutinho, Phenolic hydrogen bond donors in the formation of non-ionic deep eutectic solvents: the quest for type V DES, *Chemical Communications* 55 (2019) 10253–10256, <https://doi.org/10.1039/C9CC04846D>.
- [44] N. Schaeffer, D.O. Abranches, L.P. Silva, M.A.R. Martins, P.J. Carvalho, O. Russina, A. Triolo, L. Paccou, Y. Guinet, A. Hedoux, J.A.P. Coutinho, Non-Ideality in Thymol + Menthol Type v Deep Eutectic Solvents, *ACS Sustain Chem Eng* 9 (2021) 2203–2211, <https://doi.org/10.1021/ACSUSCHEMENG.0C07874>.
- [45] T. Phaechamud, S. Tuntarawongsa, P. Charoensuksai, Evaporation Behavior and Characterization of Eutectic Solvent and Ibuprofen Eutectic Solution, *AAPS PharmSciTech* 17 (2016) 1213–1220, <https://doi.org/10.1208/S12249-015-0459-X>.
- [46] S. Deepika, S. Juneja, Pandey, Water Miscibility, Surface Tension, Density, and Dynamic Viscosity of Hydrophobic Deep Eutectic Solvents Composed of Capric Acid, Menthol, and Thymol, *J Chem Eng Data* 67 (2022) 3400–3413, <https://doi.org/10.1021/ACS.JCED.2C00495>.
- [47] F. Kar, N. Arslan, Effect of temperature and concentration on viscosity of orange peel pectin solutions and intrinsic viscosity–molecular weight relationship, *Carbohydr Polym* 40 (1999) 277–284, [https://doi.org/10.1016/S0144-8617\(99\)00062-4](https://doi.org/10.1016/S0144-8617(99)00062-4).
- [48] S. Uribe, J.G. Sampedro, Measuring solution viscosity and its effect on enzyme activity, *Biol Proced Online* 5 (2003) 108–115, <https://doi.org/10.1251/BPO52>.
- [49] Q. Zhang, M.A. Fassihi, R. Fassihi, Delivery Considerations of Highly Viscous Polymeric Fluids Mimicking Concentrated Biopharmaceuticals: Assessment of Injectability via Measurement of Total Work Done “W T”, *AAPS PharmSciTech* 19 (2018) 1520–1528, <https://doi.org/10.1208/S12249-018-0963-X>.
- [50] S. Yadav, S.J. Shire, D.S. Kalonia, Factors affecting the viscosity in high concentration solutions of different monoclonal antibodies, *J Pharm Sci* 99 (2010) 4812–4829, <https://doi.org/10.1002/JPS.22190>.
- [51] J. Levin, H. Maibach, The correlation between transepidermal water loss and percutaneous absorption: an overview, *Journal of Controlled Release* 103 (2005) 291–299, <https://doi.org/10.1016/J.JCONREL.2004.11.035>.
- [52] M.C. Cristiano, F. Froiio, A. Mancuso, M. Iannone, M. Fresta, S. Fiorito, C. Celia, D. Paolino, In vitro and in vivo trans-epidermal water loss evaluation following topical drug delivery systems application for pharmaceutical analysis, *J Pharm Biomed Anal* 186 (2020) 113295, <https://doi.org/10.1016/j.jpba.2020.113295>.
- [53] G. Yosipovitch, C. Szolar, X.Y. Hui, H. Maibach, Effect of topically applied menthol on thermal, pain and itch sensations and biophysical properties of the skin, *Arch Dermatol Res* 288 (1996) 245–248, <https://doi.org/10.1007/BF02530092>.
- [54] Y. Chen, J. Wang, D. Cun, M. Wang, J. Jiang, H. Xi, H. Cui, Y. Xu, M. Cheng, L. Fang, Effect of unsaturated menthol analogues on the in vitro penetration of 5-fluorouracil through rat skin, *Int J Pharm* 443 (2013) 120–127, <https://doi.org/10.1016/j.ljpharm.2013.01.015>.
- [55] S. Gao, J. Singh, Mechanism of transdermal transport of 5-fluorouracil by terpenes: carvone, 1,8-cineole and thymol, *Int J Pharm* 154 (1997) 67–77, [https://doi.org/10.1016/S0378-5173\(97\)00123-3](https://doi.org/10.1016/S0378-5173(97)00123-3).
- [56] F. Xie, J.K. Chai, Q. Hu, Y.H. Yu, L. Ma, L.Y. Liu, X.L. Zhang, B.L. Li, D.H. Zhang, Transdermal permeation of drugs with differing lipophilicity: Effect of penetration enhancer camphor, *Int J Pharm* 507 (2016) 90–101, <https://doi.org/10.1016/j.ljpharm.2016.05.004>.
- [57] M. B. Brown, A. C. William, *The Art and Science of Dermal Formulation Development*, 3rd ed., 2019.
- [58] P.A. Cornwell, B.W. Barry, J.A. Bouwstra, G.S. Gooris, Modes of action of terpene penetration enhancers in human skin. Differential scanning calorimetry, small-angle X-ray diffraction and enhancer uptake studies, *Int J Pharm* 127 (1996) 9–26, [https://doi.org/10.1016/0378-5173\(95\)04108-7](https://doi.org/10.1016/0378-5173(95)04108-7).
- [59] J.A. Bouwstra, G.S. Gooris, W. Bras, D.T. Downing, Lipid organization in pig stratum corneum, *Journal Lipid Research* 36 (1995) 685–695, [https://doi.org/10.1016/S0022-2275\(20\)40054-9](https://doi.org/10.1016/S0022-2275(20)40054-9).
- [60] H.H. Agus, Terpene toxicity and oxidative stress, *Toxicology: Oxidative Stress and Dietary Antioxidants* (2021) 33–42, <https://doi.org/10.1016/B978-0-12-819092-0.00004-2>.